Mon. Not. R. Astron. Soc. **314**, 65–74 (2000)

Non-linear amplification of a magnetic field driven by cosmic ray streaming

S. G. Lucek★ and A. R. Bell★
Blackett Laboratory, Imperial College, London SW7 2BZ

Accepted 1999 December 2. Received 1999 November 22; in original form 1999 August 17

ABSTRACT

One-, two- and three-dimensional numerical results of the non-linear interaction between cosmic rays and a magnetic field are presented. These show that cosmic ray streaming drives large-amplitude Alfvénic waves. The cosmic ray streaming energy is very efficiently transferred to the perturbed magnetic field of the Alfvén waves, and the non-linear time-scale of the growth of the waves is found to be very rapid, of the order of the gyro-period of the cosmic ray. Thus, a magnetic field of interstellar values, assumed in models of supernova remnant blast wave acceleration, would not be appropriate in the region of the shock. The increased magnetic field reduces the cosmic ray acceleration time and so increases the maximum cosmic ray energy, which may provide a simple and elegant resolution to the highest energy Galactic cosmic ray problem, where the cosmic rays themselves provide the fields necessary for their acceleration.

Key words: acceleration of particles – magnetic fields – waves – cosmic rays.

Downloaded from https://academic.oup.com/mnras/article/314/1/65/1048548 by guest on 20 August 2022

1 INTRODUCTION

Current models of first-order shock acceleration (Axford, Leer & Skadron 1977; Krymsky 1977; Bell 1978; Blandford & Ostriker 1978; for reviews, see Drury 1983; Blandford & Eichler 1987) around the blast wave of a supernova remnant (SNR) have had considerable success in explaining the cosmic ray (CR) spectrum. The lifetime of the SNR, however, limits the maximum CR energy to roughly $Z \times 10^{15}$ eV, where Z is the CR charge (Lagage & Cesarsky 1983a,b), and yet a Galactic source for CRs with energies up to some 10^{18} eV, suggested by the continuity of the CR spectrum and by some evidence of Galactic plane enhancement, is favoured by many authors (for example Hillas 1984; Wdowczyk & Wolfendale 1989). However, acceleration in SNRs seems likely as supernovae are one of the few Galactic sources energetic enough to explain the CR spectrum, releasing $\sim 10^{51}$ erg around every 30 yr, corresponding to roughly 50 times the energy requirement of the CR spectrum (Volk 1987). Possible Galactic sources for CRs are also restricted by the large gyro-orbit of high-energy CRs, which requires an acceleration site of large enough extent or large enough magnetic field to contain the CRs (Hillas 1984).

Upstream of the shock, the medium is perturbed by the passage of the blast wave, and so scattering of CRs is relatively rapid. The limiting factor, on the time-scale of shock acceleration, is therefore given by the rate at which the CRs scatter downstream of the shock, isotropizing their distribution and allowing them to re-cross the shock to be further accelerated. This scattering rate is related to the CR gyro-frequency, and so dependent on the magnetic field. Lagage & Cesarsky (1983a,b), use typical interstellar medium (ISM) values for the magnetic field, and find that only with the most optimistic assumptions is it possible to accelerate CRs up to the 'knee' in the CR spectrum at some 10^{15} eV. Volk & Biermann (1988) suggest that the blast wave will not expand into a typical ISM region, but rather into the wind region of the pre-supernova star; as a result, the CRs may be accelerated to the 'knee' in the spectrum more plausibly. They further speculate that acceleration beyond this limit, up to 10^{19} eV, might be possible, although Axford (1994) points out that this requires rather larger magnetic fields than is believable.

In this paper, the amplification of a magnetic field by the streaming CRs is investigated to see whether significantly larger magnetic fields than those typically used in shock acceleration models are possible. This would ameliorate the problem of accelerating CRs to the highest galactic energies in SNR blast waves. It has long been known that streaming CRs excite Alfvén waves (Wentzel 1974; Skilling 1975a,b,c). Indeed this has been an essential part of the diffusive shock acceleration mechanism. In Bell (1978), it is these CR-excited Alfvén waves that scatter the CRs downstream of the shock, allowing them to re-cross the shock and gain energy. In Section 2, a simple linear theory is presented which shows that, in principle, the CRs can drive up extremely large-amplitude Alfvén waves. Such non-linearity, however, invalidates the assumptions of this model. In Section 3, a non-linear numerical model is presented, the results of which are discussed in Section 4. A companion paper, in preparation, discusses a somewhat restricted analytical approach to the non-linear problem. Also, Lucek & Bell (2000) (hereafter referred to

★ E-mail: s.lucek@ic.ac.uk (SGL); t.bell@ic.ac.uk (ARB)

© 2000 RAS

as Paper I) have briefly discussed the one-dimensional results alone, for a restricted set of CR distribution functions.

2 MAGNETIC FIELD GENERATION

In this section a simple linear analysis is made of the magnetic energy of Alfvén waves driven by CR streaming. In the shock rest frame, the PdV work done by the CRs on an Alfvén wave can be written as

$$\frac{dU_A}{dt} = v_A \frac{dP_{CR}}{dz}, \tag{1}$$

where P_{CR} is the CR pressure, U_A is the Alfvén wave energy density, v_A is the Alfvén velocity, and d/dt represents the convective derivative.

Expanding the convective derivative gives

$$\frac{\partial U_A}{\partial t} + v_S \frac{\partial U_A}{\partial z} = v_A \frac{\partial P_{CR}}{\partial z}, \tag{2}$$

where v_S is the shock velocity. Assuming steady state, $\partial/\partial t \rightarrow 0$, and integrating with respect to z gives

$$U_A = \frac{v_A}{v_S} P_{CR}. \tag{3}$$

Writing U_A as $\delta B^2/2\mu_0$ and v_A as $B/\sqrt{\mu_0 \rho}$ where ρ is the background fluid density gives

$$\frac{\delta B^2}{B^2} = 2 \frac{v_S}{v_A} \frac{P_{CR}}{\rho v_S^2}. \tag{4}$$

CR acceleration can be an efficient process (Volk, Drury & McKenzie 1984; Bell 1987; Falle & Giddings 1987) and so $P_{CR} \sim \rho v_S^2$. Assuming a shock moving with velocity $v_S \sim 10^4\,\mathrm{km\,s^{-1}}$, into a medium of $\sim 1\,\mathrm{proton\,cm^{-3}}$ and a magnetic field of $3 \times 10^{-6}\,\mathrm{G}$, which gives $v_S/v_A = 1500$, then a perturbed field with energies $(\delta B^2/B^2)$ up to a thousand times higher than the background field may be possible. It should be stressed that as $\delta B/B \rightarrow 1$, the problem becomes non-linear and the energy transfer becomes rather more complicated than described by equation (1). Nevertheless, equation (1) indicates a clear possibility that CRs are capable of driving strong magnetic fields, and also highlights the importance of a non-linear solution to the problem.

3 NUMERICAL MODEL

A three-dimensional, time-dependent code, CRMH3D, has been developed to examine the problem of the interaction between CRs and the background plasma. A Cartesian geometry is used. The background plasma is treated as a fluid, using the non-relativistic, ideal magneto-hydrodynamic (MHD) equations for a perfect gas. A Van Leer advection model is used, as described in Youngs (1982). This part of the code has been rigorously tested in work on jet formation, and is described in further detail in the following papers: Lucek & Bell (1996, in particular), Bell & Lucek (1995) and Lucek & Bell (1997). The CRs are treated using a particle-in-cell method (described in Birdsall & Langdon 1985). Since the number density of the CRs is very much less than the number density of particles in the fluid, both the force on the CRs and the force exerted by the CRs on the fluid are dominated by the Lorenz force between the electric and magnetic fields of the background fluid and the CR current. As the gyro-radius of the CRs is very much larger than that of the fluid ions, the electric field of the fluid can be approximated by $\boldsymbol{E} = -\boldsymbol{v}_f \times \boldsymbol{B}$, where $\boldsymbol{v}_f$ is the background fluid velocity. A fully relativistic treatment of the CR motion is implemented using a leap-frog scheme. As the time-scales of the CR motion are somewhat less than those of the background fluid, the CR time-step is resolved more finely than that of the fluid. The force of a CR on the fluid is calculated by summing the CR force over all the CR time-steps taken for each fluid time-step. In order to preserve accuracy, only a maximum of five CR time-steps are allowed for each fluid time-step. The closest numerical approach to the one used in CRMH3D that is known to the authors is presented by Zachary & Cohen (1986), who solved similar basic equations to those of CRMH3D, but used a rather different numerical technique.

4 RESULTS

4.1 Initial conditions

In the simulation, the CR streaming is represented by an isotropic distribution of CR pitch angle in a frame of reference moving with a velocity v_{iso} (in the $\hat{z}$-direction) with respect to the background fluid. In this paper results are discussed from two different CR distribution functions. The first is that, in the isotropic frame of reference, the CRs all have the same energy, with a corresponding velocity v_{CR0}. The second is that, again in the isotropic frame, the CR velocity distribution function follows a Gaussian, i.e.

$$f_{CR}(v_{CR}) \propto \exp(-v_{CR}^2/2v_{CR0}^2). \tag{5}$$

Near the shock, the CR streaming velocity is of the order of the shock velocity (McClements et al. 1996), which would be somewhat less than the gyratory velocity for high-energy CRs. Thus, in the runs presented here, a value of $v_{iso} = 0.1 v_{CR0}$ is used. So as to avoid introducing an absolute velocity scale, non-relativistic values for v_{CR0} and v_{iso} are used. A quasi-random method, which evenly distributes the CR positions and velocities from the distribution function, is used in order to ensure that the initial conditions do not create noise.

The background plasma is assumed to be uniform. A background magnetic field, of amplitude B, is applied parallel to the CR streaming direction, $\hat{z}$. A rotational Alfvén wave of amplitude δB_0 is applied, propagating along the magnetic field. The amplitude of this wave is small, $\delta B_0/B = 0.1$. It is found that the fastest growing mode in the non-linear regime has a wavelength of a fifth of the characteristic gyro-radius of the CR, $R_{CR} = m_{CR} v_{CRO}/(q_{CR} B)$ where m_{CR} and q_{CR} are the mass and charge of a CR particle. It should be noted that only CRs with velocities equal to zero parallel in the isotropic frame, will have such a gyro-radius; the average gyro-radius is 0.79 and 0.63 times the characteristic gyro-radius for the mono-energetic and Gaussian CR distribution functions respectively. As expected from linear theory, the fastest growing mode, $\lambda = 0.2 R_{CR}$, is near the resonant wavelength $\lambda = v_z \tau_{CR} \sim (v_{iso}/v_{CR0}) R_{CR}$, where v_z is the component of CR velocity parallel to the magnetic field.

In dimensionless form, the following parameters are used:

$$\rho_{fluid} = 10 \rho_{CR}, \tag{6}$$

$$v_{iso} = \frac{v_{CR0}}{10},$$

$$v_A = \frac{v_{CRO}}{100},$$

$$U_T = U_B,$$

Downloaded from https://academic.oup.com/mnras/article/314/1/65/1048548 by guest on 20 August 2022

where $\rho_{\rm fluid}$ and $\rho_{\rm CR}$ are the mass density of the background fluid and the CRs respectively, and $U_{\rm T}$ is the thermal energy density of the background plasma. The value for the Alfvén velocity, $v_{\rm A} = B/\sqrt{\mu_0 \rho_{\rm fluid}}$, and the fluid density, $\rho_{\rm fluid}$, define the magnetic field, B, and the magnetic field density, $U_B = B^2/(2\mu_0) = \rho_{\rm fluid} v_{\rm A}^2/2$. For the above parameters, the initial magnetic energy density is equal to one thousandth of the CR energy density or one tenth of the CR streaming energy. It should be noted that the above parameters represent a trade-off between choosing values that represent CRs about an SNR blast wave exactly and those that maintain the ease and accuracy of the numerical computation. Periodic boundary conditions are used in all the results presented here.

Although CRMH3D is a fully three-dimensional code, results from one-, two- and three-dimensional runs are presented here, as the symmetry of one- and two-dimensional simulations simplifies both the physics of the problem and also the interpretation of the results. In the case of the one-dimensional results, symmetry is imposed in both directions perpendicular to the background magnetic field, $\hat{\boldsymbol{x}}$ and $\hat{\boldsymbol{y}}$. Note, however, that all three components of the magnetic field, fluid velocity and CR velocity are calculated. In the two-dimensional case, symmetry is imposed only in one of the perpendicular directions, and again all three components of the fluid and CR vector quantities are calculated.

The initial conditions described above are symmetrical around both axes perpendicular to the background magnetic field. In order to break this symmetry and allow real two- and three-dimensional effects, the amplitude of the applied Alfvén wave is varied as a function of the perpendicular distances $\hat{\boldsymbol{x}}$ and $\hat{\boldsymbol{y}}$, i.e.

$$\delta B = \delta B_0 \sin^2(2\pi x/\lambda), \tag{7}$$

$$\delta B = \delta B_0 \sin^2(2\pi x/\lambda) \sin^2(2\pi y/\lambda)$$

for the two- and three-dimensional runs respectively, where λ is the wavelength of the applied Alfvén wave. It should be noted that the introduction of such a variation in the wave amplitude necessitates a similar variation in the background field, B_z, in order to satisfy $\nabla \cdot \boldsymbol{B} = 0$.

In the one-dimensional run, 200 grid cells are used in the $\hat{\boldsymbol{z}}$-direction, and the grid has a length of $R_{\rm CR}$, or five wavelengths of the dominant Alfvén wave mode. 200 CR particles per grid cell are used for the uniform CR velocity distribution case, and 1000 CR particles are used for the case where the CR velocity is drawn from a Gaussian. Since the Gaussian velocity distribution requires more CR particles to sample the distribution properly, it becomes inhibitive to use such a distribution for the two- and three-dimensional runs, which therefore only use the uniform CR velocity distribution. In the two-dimensional case, 100 grid cells are used in the $\hat{\boldsymbol{z}}$- and $\hat{\boldsymbol{x}}$-directions, and the grid has a length of $R_{\rm CR}$ in these directions. 100 CR particles are used per grid cell. In the three-dimensional case, the extent of the grid is reduced to $0.4R_{\rm CR}$, or two wavelengths of the dominant mode. 40 grid cells are used in each direction, with 100 CR particles per grid cell.

4.2 One-dimensional results

In this section, we concentrate on the results where the CRs are drawn from a Gaussian velocity distribution. Preliminary one-dimensional results for a uniform CR velocity (in the isotropic frame) are briefly discussed in detail in Paper I. We, therefore, do not consider these results here beyond comparing them with the Gaussian velocity distribution case.

Fig. 1 plots the fluid variables at successive times for the one-dimensional run. Time is plotted in units of $\omega_{\rm CR}^{-1}$, distance in units of the initial characteristic CR gyro-radius $R_{\rm CR}$, density in units of the initial CR density, and magnetic field in units of the initial background magnetic field.

The rapid growth of the Alfvén wave can clearly be seen in Fig. 1. After a CR gyro-period ($t = \tau_{\rm CR}$), the amplitude of the perturbed magnetic field is already roughly equal to the initial background field. As the perturbed field grows, the CR streaming velocity becomes effectively a gyration velocity around the perturbed field. The perturbed field grows until the gyro-radius of the CR around the perturbed field roughly equals the wavelength of the perturbation. At this point the CR gyration around the perturbed field transfers the CR streaming momentum to the background plasma, which terminates the driving of the Alfvén wave. Fig. 1 clearly shows this process. At $t = \tau_{\rm CR}$, the parallel component of the fluid momentum is small, but, as the perturbed magnetic field exceeds the background field, it rapidly grows, until half a gyro-period later, $t = 1.5\tau_{\rm CR}$, the entire CR streaming momentum has been transferred to the background plasma. From Fig. 1, it can be seen that, although the dominant frequency of the Alfvén wave is the same as is seeded in the initial conditions, other frequencies do appear.

The symmetry of the one-dimensional problem ensures that the parallel component of magnetic field is unaltered throughout the run. The wavelength of the excited Alfvén wave does not change from the initial near-resonant wave. The fluid density, fluid thermal energy density and fluid momentum parallel to the initial magnetic field, p_z, are all perturbed with a sound-like wave.

The fluid variables are very similar to the case where the CRs are mono-energetic (presented in Paper I). In particular, the growth of the dominant mode of the Alfvén wave is almost identical. The growth of the higher-frequency Alfvén waves, however, is different between the two cases, which alters the detail in Fig. 1. Also, the sound-like wave grows much more quickly in the mono-energetic CR case, with larger perturbations of ρ, $U_{\rm T}$ and p_z.

Fig. 2 shows a standard deviation calculation for the wave size, calculated from the $\hat{\mathbf{x}}$ component of the magnetic field, $\mathrm{SD}_{Bx}^2 = \sum_i [Bx(i) - \overline{Bx}]^2/n$, where the summation represents an integration over the computational grid, and n is the number of grid cells. As can be seen, the instability is fitted well by a cosh function, with an initial growth rate of $0.6\omega_{\rm CR}$ dropping to $0.45\omega_{\rm CR}$ after about $t \sim 0.3\tau_{\rm CR}$. The growth rate then remains constant, even after the perturbed magnetic field has grown to non-linear values (at $t \sim \tau_{\rm CR}$), right up to the termination of the wave excitation process. The growth rates obtained are roughly consistent with linear theory. For example, Blandford & Eichler (1987) obtain a growth rate for a monochromatic Alfvén wave of $\sigma \sim (\rho_{\rm CR}/\rho_{\rm fluid})(v_{\rm iso}/v_{\rm A} - 1)\omega_{\rm CR}$ where $\omega_{\rm CR}$ is the gyro-frequency of the CR. For the initial conditions used here, this gives a growth rate of $0.9\omega_{\rm CR}$. It should be noted that the Blandford & Eichler (1987) linear theory assumes a different CR distribution function from that used here, and so exact agreement of the growth rates is not expected.

Since the initial near-resonant wavelength is so clearly the dominant Alfvén wave mode, even at later times, and this mode growth is very similar in both the mono-energetic CR case and the Gaussian CR velocity distribution case, the SD measurement plotted in Fig. 2 is almost identical for the mono-energetic CR case.

Fig. 3 shows the energy plot for the one-dimensional run. The CR streaming energy is calculated from the bulk z momentum of the CR, $E_{\rm CRstream} = (\sum p_{\rm CRz})^2/(2M_{\rm CR})$, where $M_{\rm CR}$ is the total

Downloaded from https://academic.oup.com/mnras/article/314/1/65/1048548 by guest on 20 August 2022

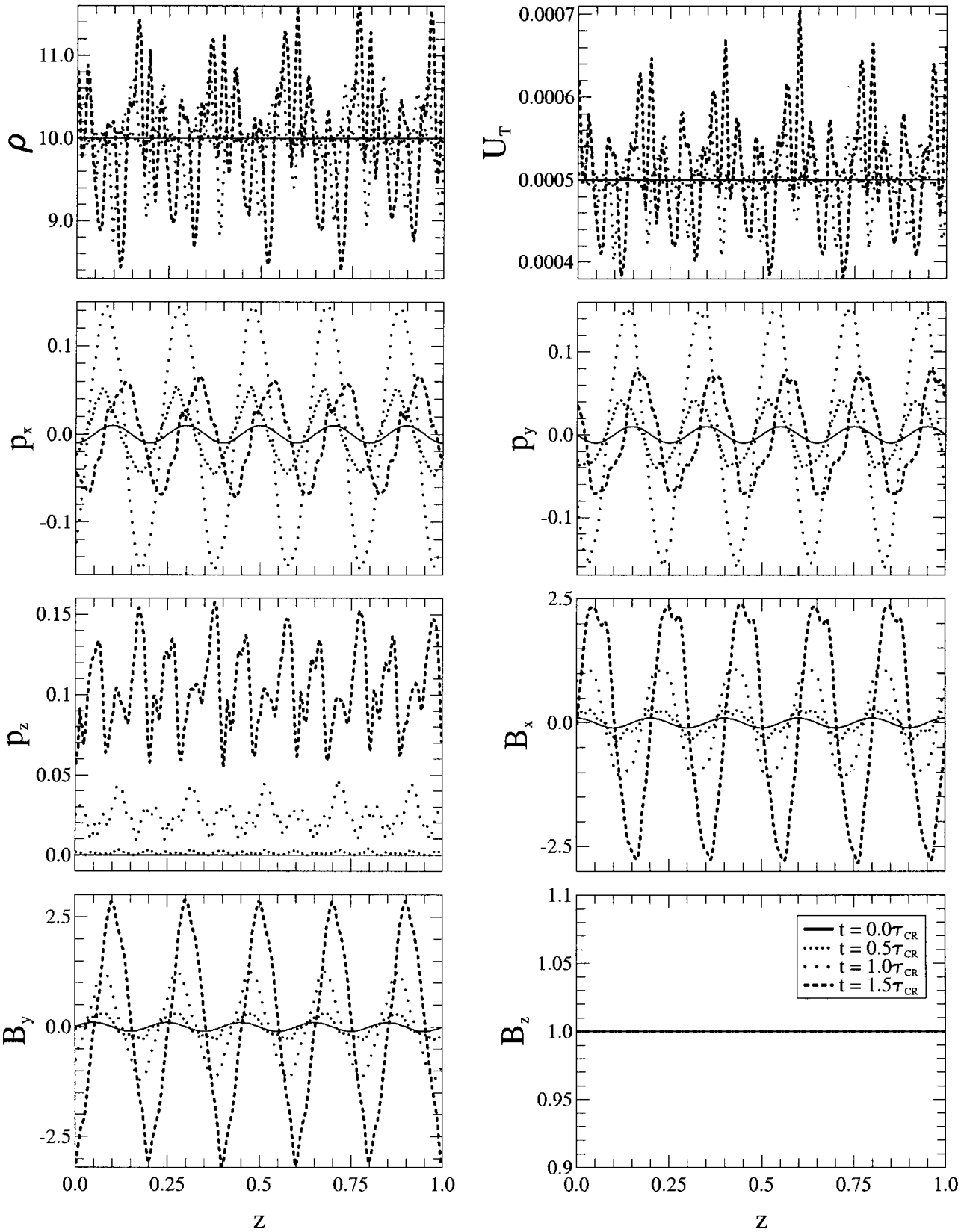

Figure 1. Plot of the fluid variables at successive times for the one-dimensional run. ρ represents the fluid density, U_T the fluid thermal energy density, p_x, p_y and p_z the two perpendicular and one parallel component (with respect to the initial magnetic field) of fluid momentum density, and B_x, B_y and B_z the three components of magnetic field. Length is in units of the characteristic CR gyro-radius and time in units of the inverse CR gyro-frequency.

Downloaded from https://academic.oup.com/mnras/article/314/1/65/1048548 by guest on 20 August 2022

mass of the CR and the summation represents the total CR momentum in the $\hat{\mathbf{z}}$-direction. The peak magnetic field energy, 0.004, at a time $1.5\tau_{CR}$ represents 80 per cent of the initial CR streaming energy. The second panel of Fig. 3 shows the maximum amplitude of the magnetic field. This grows to almost four times the initial background field, or 40 times the initial magnetic field perturbation. The third panel shows the momentum of the CR and the fluid parallel to the initial background field. It can clearly be seen that the driving of the Alfvén wave is terminated when the CR streaming momentum has been transferred to the plasma. Fig. 3 also shows the transfer of the streaming momentum backwards and forwards between the CR and the fluid, and the corresponding increases and decreases of the magnetic field energy. As discussed above, this arises because, as the perturbed magnetic field becomes large, the CR streaming velocity becomes effectively a gyratory motion around the perturbed field. The transfer of streaming momentum backwards and forwards between the CR and the fluid is so large because the CR gyratory motion around the perturbed field is largely in phase, since the CRs driving the Alfvén wave start with similar streaming velocities.

Again, since the growth of the dominant mode is almost identical in both the mono-energetic CR case and the Gaussian CR velocity distribution case, so the energy plot for the mono-energetic CR case is almost identical to Fig. 3.

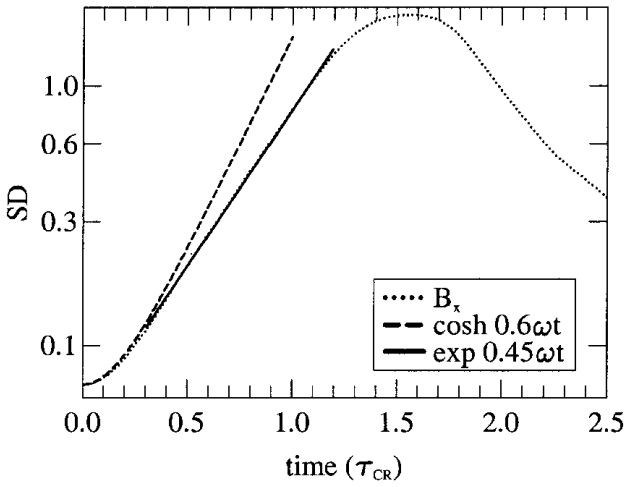

Figure 2. Plot of the amplitude of the magnetic field of the Alfvén wave, measured as the standard deviation of B_x.

4.3 One-dimensional results with artificial CR acceleration

In reality, the acceleration of CRs at the shock is a continuous process, and so the sudden input of streaming CRs on a relatively unperturbed medium is a restricted model. Rapid isotropization of the CR is not likely near the shock, and so acceleration of the CRs at the shock will maintain a gradient in the CR streaming pressure which drives the Alfvén waves. To simulate this crudely, and also to give some idea of the form of the steady-state solution to the problem, an artificial, constant acceleration is applied to all the CRs. This acceleration acts in the streaming ($\hat{\mathbf{z}}$) direction, parallel

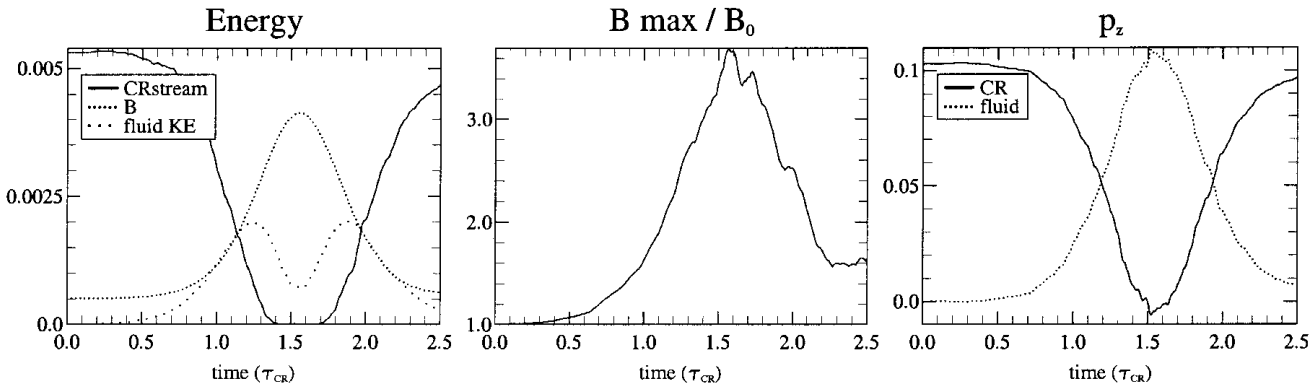

Figure 3. Energy, peak magnetic field and momentum parallel to the initial background magnetic field for the one-dimensional run.

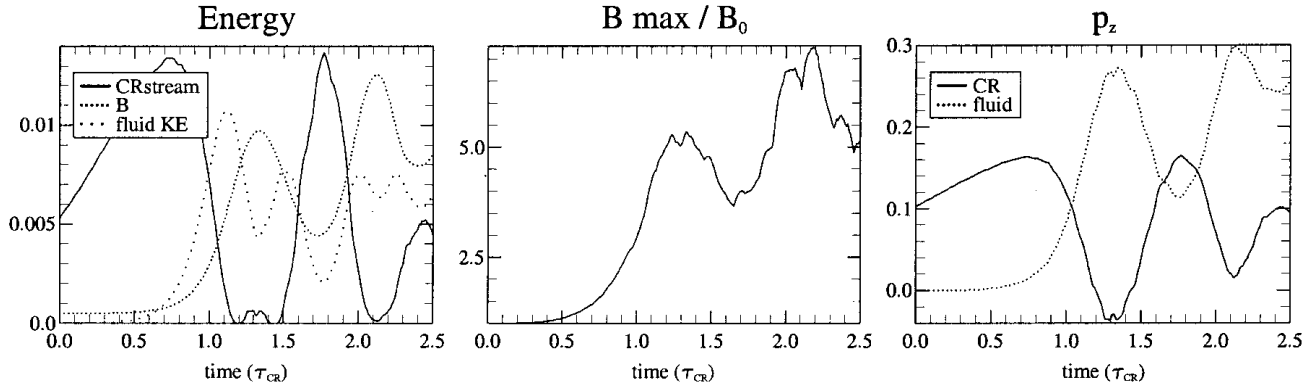

Figure 4. Energy, peak magnetic field and momentum parallel to the initial background magnetic field for the one-dimensional run with artificial acceleration applied to the CRs.

Downloaded from https://academic.oup.com/mnras/article/314/1/65/1048548 by guest on 20 August 2022

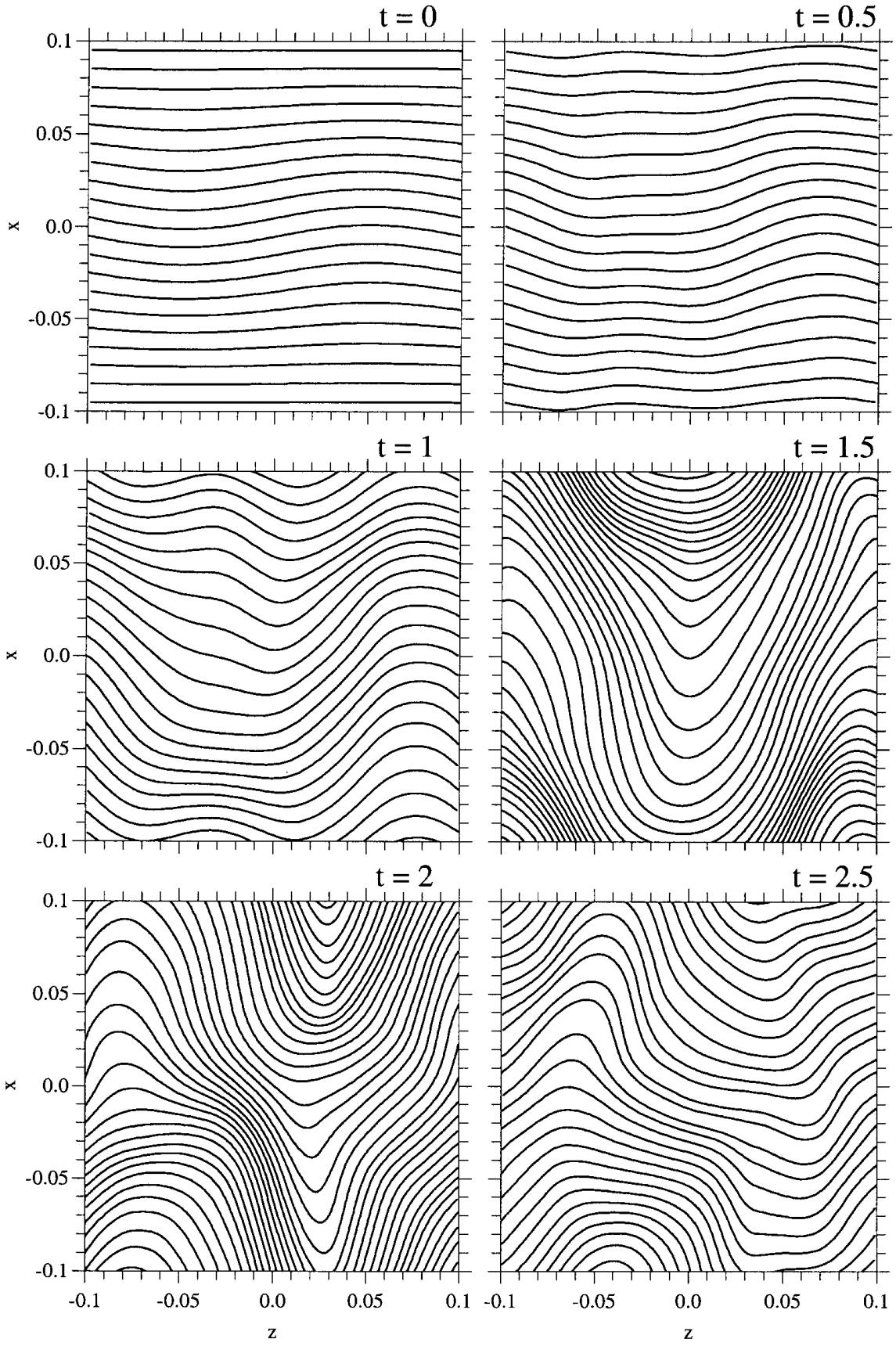

Figure 5. Plot of the magnetic field lines at successive times for the two-dimensional run.

Downloaded from https://academic.oup.com/mnras/article/314/1/65/1048548 by guest on 20 August 2022

to the initial background magnetic field. Since the transfer of energy from the streaming CRs to the Alfvén wave is rapid, of the order of the gyro-period of the CRs, the acceleration needs to be large. The acceleration applied corresponds to an increase equal to the initial CR streaming velocity over the initial CR gyro-period. The Gaussian CR velocity distribution case is considered.

Fig. 4 shows the energy plot for the one-dimensional run with artificial CR acceleration. Energy is transferred from the streaming CRs to the Alfvén wave in a similar fashion to the one-dimensional case without artificial CR acceleration. The peaks in energy in the magnetic field at $t \sim 1.3\tau_{CR}$ and $\sim 2.1\tau_{CR}$ both represent 50 per cent of the total CR streaming energy, i.e. the initial CR streaming energy and the energy supplied to the CR through the artificial CR acceleration. At these times the total CR streaming energy is roughly four and five times, respectively, the initial CR streaming energy. The Alfvén wave grows in a similar way to the case where no acceleration is applied, although the exponential growth rate remains at $0.6\omega_{CR}$ until all the initial CR streaming momentum has been transferred to the background fluid at $t \sim 1.3\tau_{CR}$. Fig. 4 clearly shows that the artificial acceleration does indeed maintain the CR streaming, and continues to drive the Alfvén wave even after the initial CR streaming momentum has been transferred to the background plasma. This indicates that the mechanism for magnetic field amplification is not dependent on a sudden impulse of streaming CRs, but continues to work for a steady flux of streaming CRs.

Since the CRs are being accelerated, more energy is transferred to the Alfvénic and sound-like perturbations, resulting in steeper energy and density gradients. In particular, the gradients associated with the sound-like waves are difficult to resolve at later times. To retain numerical accuracy the sound-like waves are damped by increasing the initial fluid thermal energy density ($U_T = 10U_B$) and hence the sound speed. The growth of the Alfvén wave, up to the point where both cases are numerically accurate, is unaltered by this change.

Fig. 4 also shows the transfer of the streaming momentum backwards and forwards between the CR and the fluid. This corresponds, however, to a smaller fraction of magnetic field energy than in the case without artificial CR acceleration. Also, the amplitude of oscillation in the magnetic field energy is smaller at later times than at first. This indicates that as time progresses the CR gyration around the perturbed magnetic field becomes less coherent. Nevertheless, the artificial CR acceleration continues to drive the growth of the Alfvén wave.

4.4 Two-dimensional results

It is clear that in the one-dimensional results the energy in the magnetic field is dominated by the initially near-resonant Alfvén wave mode, and that the growth of this mode is almost identical in the mono-energetic CR case and in the case of a Gaussian CR velocity distribution. Since, in this paper, we are primarily concerned with the energy transfer from the streaming CRs to the background magnetic field and the Gaussian CR velocity distribution is computationally more expensive, we consider only the mono-energetic CR case for the results in two and three dimensions.

Fig. 5 shows the magnetic field lines plotted at successive times for the two-dimensional run. Only the central fifth of the computational region is shown, corresponding to one wavelength of the dominant Alfvén wave mode. Because this mode is so dominant throughout the run, the magnetic field lines are largely periodic, and the regions beyond that plotted in Fig. 5 are very similar. Unlike the one-dimensional case the perturbation increases all three components of the magnetic field. It can be seen that the dominant wavelength of the excited Alfvén wave does not change from the initial near-resonant wave, even though the perturbed field has become large.

Fig. 6 shows the energy plot for the two-dimensional run. The transfer of energy from the streaming CRs to the magnetic field is very similar to the one-dimensional case, with the energy in the magnetic field reaching ~75 per cent of the CR streaming energy. The Alfvén wave grows almost exactly like the one-dimensional case, with the same exponential growth rate. Without the symmetry imposed in the one-dimensional run, however, the gyration of the CRs around the perturbed field is not so well-ordered, and so not all the CR streaming energy is transferred back from the magnetic field. It is remarkable that, despite the very different behaviour between the magnetic field of the one- and two-dimensional cases, the transfer of energy between the streaming CRs and the background field is very similar.

4.5 Two-dimensional results with artificial CR acceleration

Fig. 7 shows the energy plot for the two-dimensional run when an artificial acceleration is applied to the CRs. Again, for greater numerical accuracy, the initial thermal pressure is increased ($U_T = 10U_B$) to slow the growth of the sound-like wave. The energy transfer is very similar to the one-dimensional case, with

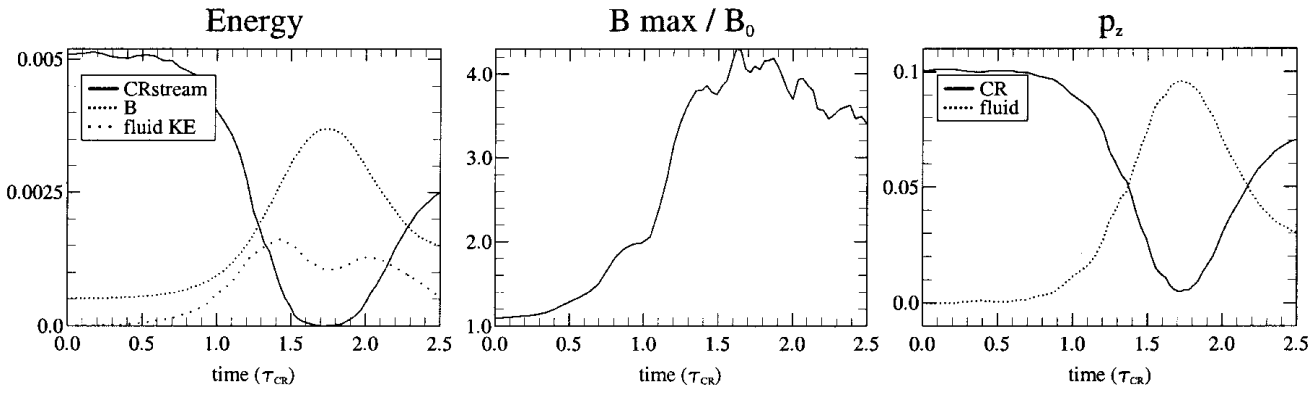

Figure 6. Energy, peak magnetic field and momentum parallel to the initial background magnetic field for the two-dimensional run.

Downloaded from https://academic.oup.com/mnras/article/314/1/65/1048548 by guest on 20 August 2022

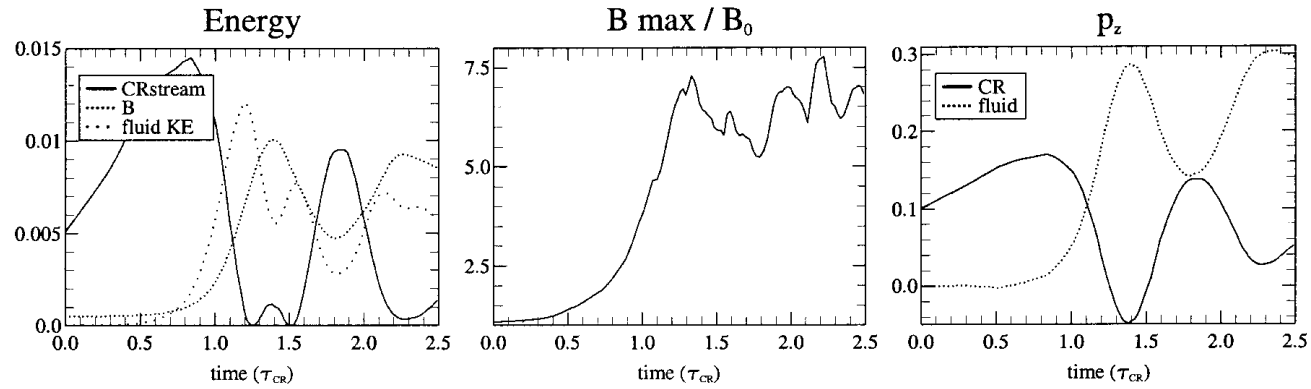

Figure 7. Energy, peak magnetic field and momentum parallel to the initial background magnetic field for the two-dimensional run with artificial acceleration applied to the CRs.

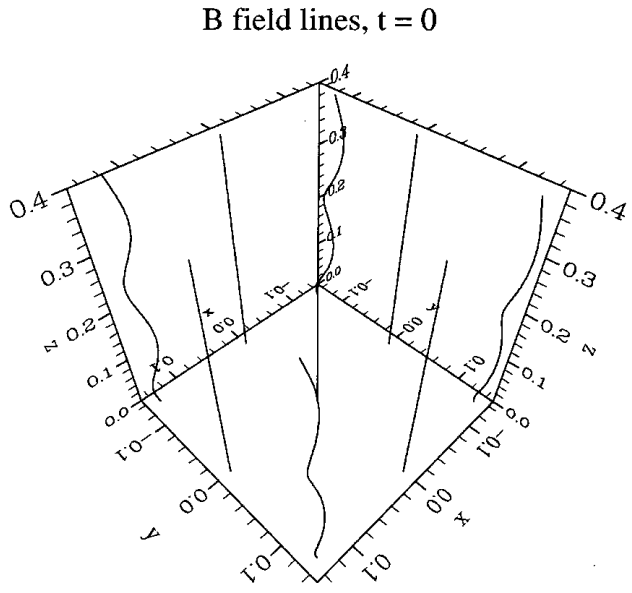

Figure 8. Magnetic field lines at $t = 0$ for the three-dimensional run.

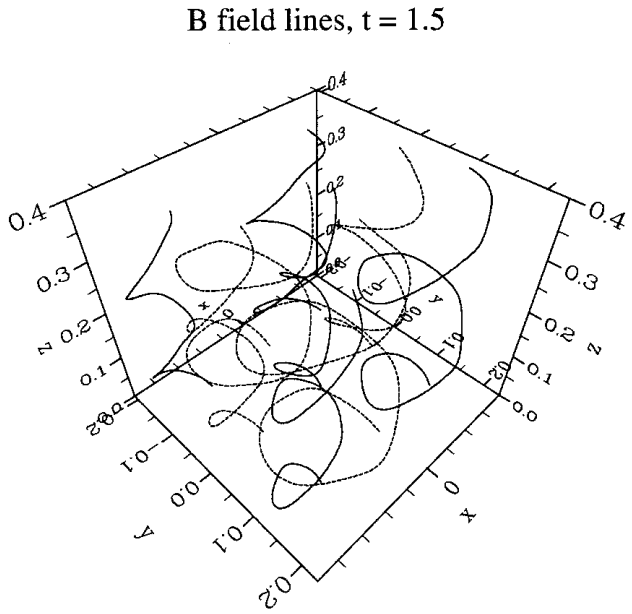

Figure 9. Magnetic field lines after 1.5 CR gyrations for the three-dimensional run.

about 50 per cent of the total CR streaming energy transferred to the magnetic field at $t = 1.4\tau_{CR}$. Unlike the one-dimensional case, it is not clear in the two-dimensional case what happens after all the initial CR streaming momentum is passed to the plasma. Since the CRs are being accelerated, this means there is more energy transferred to the Alfvénic and sound-like perturbations, resulting in steeper energy and density gradients which make resolution of the problem in two dimensions difficult. Hence the code is unreliable after $\sim 1.8\tau_{CR}$. Nevertheless, at the peak magnetic field energy at $t = 1.4\tau_{CR}$ the magnetic field energy is already twice the original CR streaming energy, and so it is clear that some of the driving of the magnetic field is achieved by the steady acceleration of streaming CRs, rather than being driven entirely by the initial impulse of streaming CRs.

4.6 Three-dimensional results

The magnetic field line plots for the three-dimensional run (Figs 8, 9 and 10) clearly show the Alfvén wave growth. Also, it is clear that the fields are fully three-dimensional. The energy plot (Fig. 11) again shows a transfer of energy from the streaming CRs to the magnetic field similar to that in the one-dimensional case. The peak magnetic field energy represents 65 per cent of the initial CR streaming energy. Like the one-dimensional case, the Alfvén wave size is initially well-fitted by cosh $0.6\omega_{CR}$, although later the growth rate drops to $0.33\omega_{CR}$, compared with $0.45\omega_{CR}$ in the one-dimensional case.

5 CONCLUSIONS

In this paper numerical results have been presented which show that CR streaming drives large-amplitude Alfvén waves with magnetic fields that dominate the background field. The growth rates from linear theory persist well into the non-linear regime. The driving of the waves is only stopped when the perturbed field becomes large and the streaming CRs begin to gyrate about the perturbed field, transferring their streaming momentum to the background plasma. The rapid driving of the waves, coupled with the fact that the termination of the driving mechanism is effected through the perturbed field, means that the energy transfer to the

Downloaded from https://academic.oup.com/mnras/article/314/1/65/1048548 by guest on 20 August 2022

magnetic field is not highly dependent on the details of the mechanism. It is quite remarkable that the clear differences in the behaviour of the magnetic field in the one-dimensional case, compared with that shown in the two- and three-dimensional cases, do not significantly alter the transfer of energy between the CR streaming and the magnetic field. Also, in Section 4.2 it is found that the growth of both the non-resonant Alfvén wave modes and the sound-like wave modes is different for the two initial CR distributions considered. The growth of the near-resonant Alfvén wave mode, however, is unaffected by these changes, and the energy transfer, dominated by this mode, is almost identical.

It should be stressed that the results discussed here do not present a full model for the transfer of SNR energy to the CRs and thence to the magnetic field, and so concrete predictions for the likely magnetic fields, and the highest energies possible for CR scattering in such fields, are not yet possible. Also, the model presented here, representing the sudden input of streaming CRs on a relatively unperturbed medium, is restricted; although the introduction of an artificial acceleration represents, in a simple fashion, the maintenance of the gradient in the CR pressure by the acceleration of the CR at the shock. Despite these caveats, the model allows a simple, and admittedly crude, estimate of the final magnetic field that might be possible. In this paper the CR streaming energy has been found to be very efficiently transferred to the magnetic field. Since this transfer occurs quickly, at least as rapidly as the rate of CR acceleration at the shock, then it might be expected that the magnetic field energy should be roughly equal to the total CR streaming energy. For efficient CR acceleration at the shock, the CR pressure (or energy density) is given by $P_{\rm CR} \sim \rho v_{\rm S}^2$, where $\rho v_{\rm S}^2$ represents the shock energy. The CR streaming energy density, non-relativistically, is given by $(v_{\rm S}^2/c^2)P_{\rm CR}$, where $v_{\rm S}$ is the CR streaming velocity, equal to the shock velocity. For highly relativistic particles this becomes $(v_{\rm S}/c)P_{\rm CR}$, although this does not greatly change the final magnetic field estimate. Thus, setting the magnetic field energy density to the CR streaming energy density gives $B^2 \sim \mu_0(v_{\rm S}^2/c^2)\rho v_{\rm S}^2$, resulting in a magnetic field of $B \sim (v_{\rm S}^2/c^2)\sqrt{\mu_0\rho}\,c$. Using $v_{\rm S}/c \sim 0.1$ and assuming a medium of $\rho \sim 1$ proton cm^{-3}, this gives a magnetic field of up to 1000 μG, a factor of a 1000 more than that used by Lagage & Cesarsky (1983a,b).

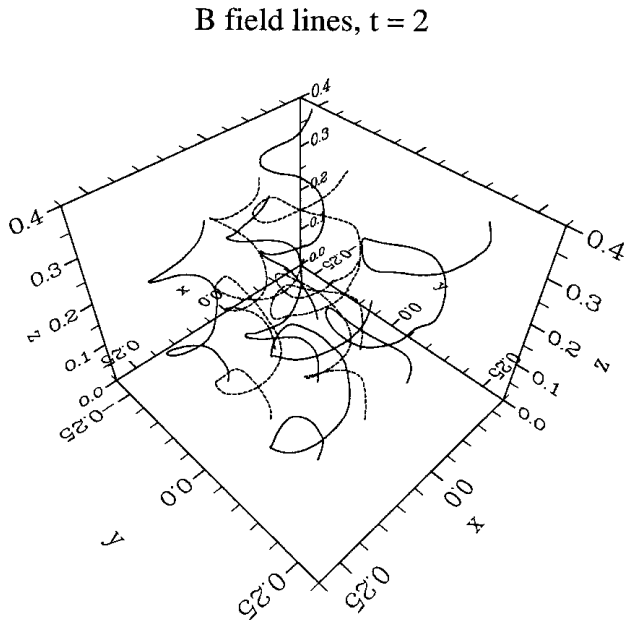

Figure 10. Magnetic field lines after 2 CR gyrations for the three-dimensional run.

It is important that the length-scales of the magnetic turbulence, driven by the CR streaming, should correspond to those that will scatter the CR efficiently, otherwise there would be no increase in the acceleration rate for the CR. It has been discussed in Section 4.2 that, even though the near-resonant Alfvén wave mode has a wavelength somewhat less than that of the initial gyro-radius of the CR, the increase in magnetic field results in CR gyro-radii comparable to the wavelength of the dominant Alfvén wave mode. Thus, one would expect efficient scattering of the CRs in the magnetic fields generated in this model, which is important if the increased magnetic field is to increase the acceleration rate.

In the non-linear results presented here, it is found that the CR streaming strongly drives the Alfvén waves. The transfer of CR streaming energy to magnetic field energy is very efficient. This amplification of the magnetic field ameliorates the problem of achieving the highest energy Galactic CRs in diffusive acceleration in SNR blast waves by reducing the acceleration time of the CRs. This may provide a simple and elegant resolution to the high-energy Galactic cosmic ray problem where the cosmic rays themselves provide the fields necessary for their own acceleration.

ACKNOWLEDGMENTS

The authors thank PPARC for funding this project (grant GR/L 21129). They also gratefully acknowledge helpful discussions with colleagues in the Plasma Physics and Astrophysics groups at

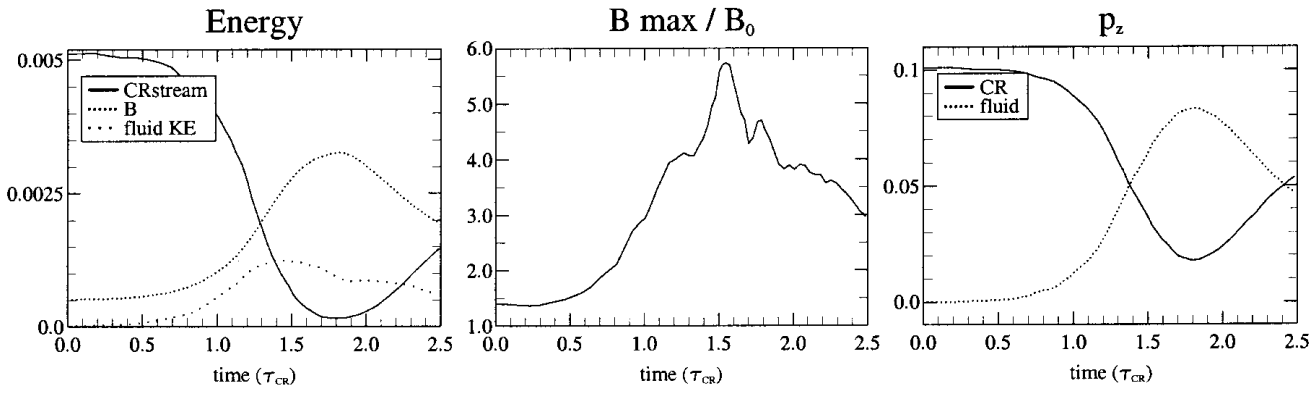

Figure 11. Energy, peak magnetic field and momentum parallel to the initial background magnetic field for the three-dimensional run.

Downloaded from https://academic.oup.com/mnras/article/314/1/65/1048548 by guest on 20 August 2022

Imperial College, and also with workers in the European network for research in AstroPlasmaPhysics, especially Luke Drury.

REFERENCES

Axford W. I., 1994, ApJS, 90, 937
Axford W. I., Leer E., Skadron G., 1977, in eds, Proc. 15th Int. Cosmic Ray Conf., p. 132
Bell A. R., 1978, MNRAS, 182, 147
Bell A. R., 1987, MNRAS, 225, 615
Bell A. R., Lucek S. G., 1995, MNRAS, 277, 1327
Birdsall C. K., Langdon A. B., 1985, Plasma Physics Via Computer Simulation. McGraw-Hill, New York
Blandford R. D., Eichler D., 1987, Phys. Rep., 154, 1
Blandford R. D., Ostriker J. P., 1978, ApJ, 221, L29
Drury L. O'C., 1983, Rep. Prog. Phys., 46, 973
Falle S. A. E. G., Giddings J. R., 1987, MNRAS, 225, 399
Hillas A. M., 1984, ARA&A, 22, 425
Krymsky G. F., 1977, Dokl. Akad. Nauk. SSSR, 234, 1306
Lagage P. O., Cesarsky C., 1983, A&A, 118, 223
Lagage P. O., Cesarsky C., 1983, A&A, 125, 249
Lucek S. G., Bell A. R., 1996, MNRAS, 281, 245
Lucek S. G., Bell A. R., 1997, MNRAS, 290, 327
Lucek S. G., Bell A. R., 2000, in Berry D., ed., Astrophysical Dynamics Conf., Ap&SS, in press (Paper I)
McClements K. G., Dendy R. O., Drury L. O'C., Duffy P., 1996, MNRAS, 280, 219
Skilling J., 1975, MNRAS, 172, 557
Skilling J., 1975, MNRAS, 173, 245
Skilling J., 1975, MNRAS, 173, 255
Volk H. J., 1987, in eds, Proc. 20th Int. Cosmic Ray Conf., p. 157
Volk H. J., Biermann P. L., 1988, ApJ, 333, L65
Volk H. J., Drury L. O'C., McKenzie J. F., 1984, A&A, 130, 19
Wdowczyk J., Wolfendale A. W., 1989, Ann. Rev. Nucl. Part. Sci., 39, 43
Wentzel D. G., 1974, ARA&A, 12, 71
Youngs D. L., 1982, in Morton K. W., Baines M. J., eds, Numerical Methods in Fluid Dynamics. Academic Press, New York, p. 273
Zachary A. L., Cohen B. I., 1986, J. Comput. Phys., 66, 469

This paper has been typeset from a TEX/LATEX file prepared by the author.

Downloaded from https://academic.oup.com/mnras/article/314/1/65/1048548 by guest on 20 August 2022